



Lithologic controls on landscape dynamics and aquatic species evolution in post-orogenic mountains

Sean F. Gallen¹

Department of Earth Sciences, ETH-Zurich, Switzerland

ARTICLE INFO

Article history:

Received 3 December 2017

Received in revised form 9 March 2018

Accepted 17 April 2018

Available online 27 April 2018

Editor: J.-P. Avouac

Keywords:

landscape evolution

post-orogenic

drainage basin dynamics

erodibility

biodiversity

ABSTRACT

Determining factors that modify Earth's topography is essential for understanding continental mass and nutrient fluxes, and the evolution and diversity of species. Contrary to the paradigm of slow, steady topographic decay after orogenesis ceases, nearly all ancient mountain belts exhibit evidence of unsteady landscape evolution at large spatial scales. External forcing from uplift from dynamic mantle processes or climate change is commonly invoked to explain the unexpected dynamics of dead orogens, yet direct evidence supporting such inferences is generally lacking. Here I use quantitative analysis of fluvial topography in the southern Appalachian Mountains to show that the exhumation of rocks of variable erosional resistance exerts a fundamental, autogenic control on the evolution of post-orogenic landscapes that continually reshapes river networks. I characterize the spatial pattern of erodibility associated with individual rock-types, and use inverse modeling of river profiles to document a ~150 m base level fall event at 9 ± 3 Ma in the Upper Tennessee drainage basin. This analysis, combined with existing geological and biological data, demonstrates that base level fall was triggered by capture of the Upper Tennessee River basin by the Lower Tennessee River basin in the Late Miocene. I demonstrate that rock-type triggered changes in river network topology gave rise to the modern Tennessee River system and enhanced erosion rates, changed sediment flux and dispersal patterns, and altered bio-evolutionary pathways in the southeastern U.S.A., a biodiversity hotspot. These findings suggest that variability observed in the stratigraphic, geomorphic, and biologic archives of tectonically quiescent regions does not require external drivers, such as geodynamic or climate forcing, as is typically the interpretation. Rather, my findings lead to a new model of inherently unsteady evolution of ancient mountain landscapes due to the geologic legacy of plate tectonics.

© 2018 Elsevier B.V. All rights reserved.

1. Introduction

The development of topography on Earth influences the flux and routing of surface water, sediment, and organic matter to the world's oceans (Milliman and Syvitski, 1992; Summerfield and Hulton, 1994; France-Lanord and Derry, 1997; Battin et al., 2008), affects feedbacks between the solid Earth and atmosphere (Molnar and England, 1990; Raymo and Ruddiman, 1992), and alters the evolution and diversity of plant and animal species (Mayden, 1988; Waters et al., 2001; Hoorn et al., 2010). While the dominant mechanisms that drive topographic change in tectonically active settings, such as rock uplift and climate (Molnar and England, 1990), are clear, those that govern landscape evolution in tectonically quiescent mountains remain ambiguous. The conventional view of post-orogenic landscape evolution is one of slow, steady reduc-

tion in mean elevation, erosion rate, and topographic relief (Davis, 1899). However, most dead orogens preserve evidence of variable sediment flux and erosion rate and periods of topographic rejuvenation long after tectonics ends (Pazzaglia and Brandon, 1996; Hancock and Kirwan, 2007; Galloway et al., 2011; Gallen et al., 2013; Miller et al., 2013; Tucker and van der Beek, 2013). Most researchers now agree that topographic evolution in dead orogens is unsteady, although the underlying driving mechanisms remain poorly understood.

With the availability of high-resolution tomographic imaging of the Earth's mantle and global mantle convection models, uplift via dynamic topography or removal of lithospheric material has emerged as a process commonly invoked to explain topographic changes in tectonically inactive settings (Pazzaglia and Brandon, 1996; Gallen et al., 2013; Miller et al., 2013; Rowley et al., 2013; Liu, 2014; Biryol et al., 2016). Alternatively, climate change is often called upon to explain enigmatic evidence of landscape change under the assumption that a transition to a Quaternary-like climate ~3–4 Ma enhanced erosional efficiency on a global scale

E-mail address: sean.gallen@colostate.edu.¹ Current affiliation: Department of Geosciences, Colorado State University.

(Molnar and England, 1990; Hancock and Kirwan, 2007). The majority of studies rely on conceptual arguments and approximate spatial and temporal coincidence of landscape change with seismic wave velocity anomalies in the mantle or shifts in climate proxy data, whereas others use more sophisticated geodynamic or climate models to support a favored interpretation. However, in most cases such arguments are circumstantial, and do not provide particularly compelling support for either mechanism.

Landscapes in all dead orogens evolve on complex and spatially variable, but predictable geology. Links between topographic form and rock-type have long been observed (Hack, 1960; Mills, 2003), and spatially variable bedrock erodibility has been invoked as an attempt to explain changes in the retreat rate of passive margin escarpments (Gunnell and Harbor, 2010; Naeser et al., 2016). However, only recently have modeling studies shown that landscape evolution is surprisingly dynamic when rivers incise through rocks of variable erosional resistance (Forte et al., 2016) and that spatial variations of rock-types common in ancient mountain belts may play a role in post-orogenic topographic change (Tucker and van der Beek, 2013). Nevertheless, the potentially important role of rock-type as an autogenic driver of transient landscape evolution and river network reorganization, which modifies sediment dispersal patterns and fragments aquatic ecosystems, enriching biodiversity (Mayden, 1988; Waters et al., 2001; Near and Keck, 2005; Kozak et al., 2006; Rahel, 2007; Hoorn et al., 2010), remains largely unexplored in natural settings.

Here, I perform a quantitative geomorphology study of the southern Appalachian Mountains, where the last phase of tectonic activity ended >200 Ma (Hatcher, 1989), to elucidate the role of variable erodibility associated with different rock units on unsteady landscape evolution and drainage basin dynamics in post-orogenic regions. In this study, first, I quantify the impact of rock-type on topographic form and landscape response times, and use a formal linear inversion of river profiles to extract the history of transient landscape evolution; second, I use rock-type as a proxy for the spatial distribution of erodibility to elucidate the mechanisms driving transient landscape evolution and drainage basin dynamics in post-orogenic settings. I focus my study on the >105,000 km² Tennessee River Basin that flows westward from the eastern continental divide over rock-types common to all ancient mountain settings, and hosts the most diverse freshwater fish fauna in North America (Etnier and Starnes, 1993), making it an ideal setting to study the processes that shape post-orogenic topography and give rise to elevated biodiversity (Fig. 1).

2. Description of the study area

The Appalachians were built during a series of collisional episodes during the Paleozoic that ended with closure of the Iapetus Ocean during the Alleghany Orogeny (Hatcher, 1989). The former mountain range was rifted in the Late Triassic during opening of the North Atlantic and has since been tectonically inactive (Hatcher, 1989). The legacy of Paleozoic mountain building, Mesozoic rifting, and the subsequent passive margin history of eastern North America is strongly expressed in the modern landscape, and forms the basis for the classification of distinct physiographic provinces (Reed et al., 2005) (Fig. 1). Mesozoic to Cenozoic marine and terrestrial sediments of the Coastal Plain record the rifting and passive margin history. High-to-mid grade metamorphic rocks of the low-relief Piedmont and high-relief Blue Ridge represent the former hinterland of the Alleghany Orogen. Sedimentary units of the Alleghany fold-thrust belt and foreland basin define the Valley and Ridge province, and Appalachian and Interior Low Plateau provinces, respectively (Fig. 1a).

The Tennessee River basin spans the Blue Ridge, Valley and Ridge, and Appalachian and Interior Low Plateaus, and is divided

into the Upper and Lower Tennessee basins that are connected by the Tennessee River Gorge near the city of Chattanooga, TN (Fig. 1). The axis of the main valley of the Upper Tennessee River basin is oriented roughly south-southwest before taking an abrupt westward turn as it enters the Tennessee River Gorge (Fig. 1). The river then flows westward through the Lower Tennessee basin, turns north joining the Ohio and Mississippi rivers before flowing southward and ultimately discharging into the Gulf of Mexico, nearly 3000 river kilometers from its headwaters (Fig. 1a).

For more than a century, geologists, physical geographers, and biologists have pondered the curious, long westward course of the Tennessee River, debating whether the Lower Tennessee River captured a paleo-Upper Tennessee River, known as the Appalachian River, diverting it from a more direct southerly route to the Gulf of Mexico via the Mobile basin (Hayes and Campbell, 1894; Simpson, 1900; Johnson, 1905) (Fig. 1a, b). Geologic studies remain ambiguous with evidence cited both for and against major shifts in flow direction of the Tennessee River (Hayes and Campbell, 1894; Johnson, 1905; Mills and Kaye, 2001; Mills, 2005). Phylogenetic studies in the southeastern U.S.A. indicate that freshwater faunal vicariance and dispersal events have been common during the late Cenozoic, implying reorganization of river networks; however, without conclusive corroborating geologic evidence, the timing and mechanisms that facilitated drainage rearrangement are debated (Mayden, 1988; Near and Keck, 2005; Kozak et al., 2006). Resolution of this controversy demands compelling evidence for or against capture of the Upper Tennessee basin, and if such evidence exists, determining that timing of capture and the mechanism(s) capable of reshaping of river networks in the absence of tectonic forcing. The Tennessee River controversy, thus, represents a microcosm of the broader questions regarding the drivers of dynamic landscape evolution in post-orogenic settings.

3. Fluvial geomorphology of the Upper Tennessee River basin

Capture of the hypothesized Appalachian river should leave a signal of discrete base level fall on the upstream fluvial network (the Upper Tennessee drainage basin), provided the response time of the river system is longer than the time since capture. Therefore to evaluate the Appalachian River hypothesis, I perform a quantitative analysis of fluvial topography in the Upper Tennessee basin to determine if it preserves a signature of base level fall consistent with river capture at its present-day outlet. For this analysis, I use 1-arc second (~30 m) Shuttle Radar Topography Mission (SRTM) digital topography. River networks are extracted based on a threshold drainage area of 5 km² and analyzed using TopoToolbox version 2.1 (see details below) (Schwanghart and Scherler, 2014). In this section, I first characterize the basic river profile morphology using standard river profile analysis; I then quantify the spatial variability in rock-type related erodibility in the drainage basin; finally, after controlling for the influence of spatially variable erodibility, I test for the signature of river capture in the Upper Tennessee River basin using a formal linear inversion of fluvial topography that allows for characterization of the base level fall history.

3.1. River profile analysis

River incision, E , into bedrock is typically modeled as a function of upstream contributing drainage area and channel gradient and, assuming detachment-limited conditions, can be expressed as (Howard, 1994):

$$E = KA^m S^n, \quad (1)$$

where A is the upstream drainage area, S is local channel slope (dz/dx), K is a dimensional erodibility coefficient, and m and n are

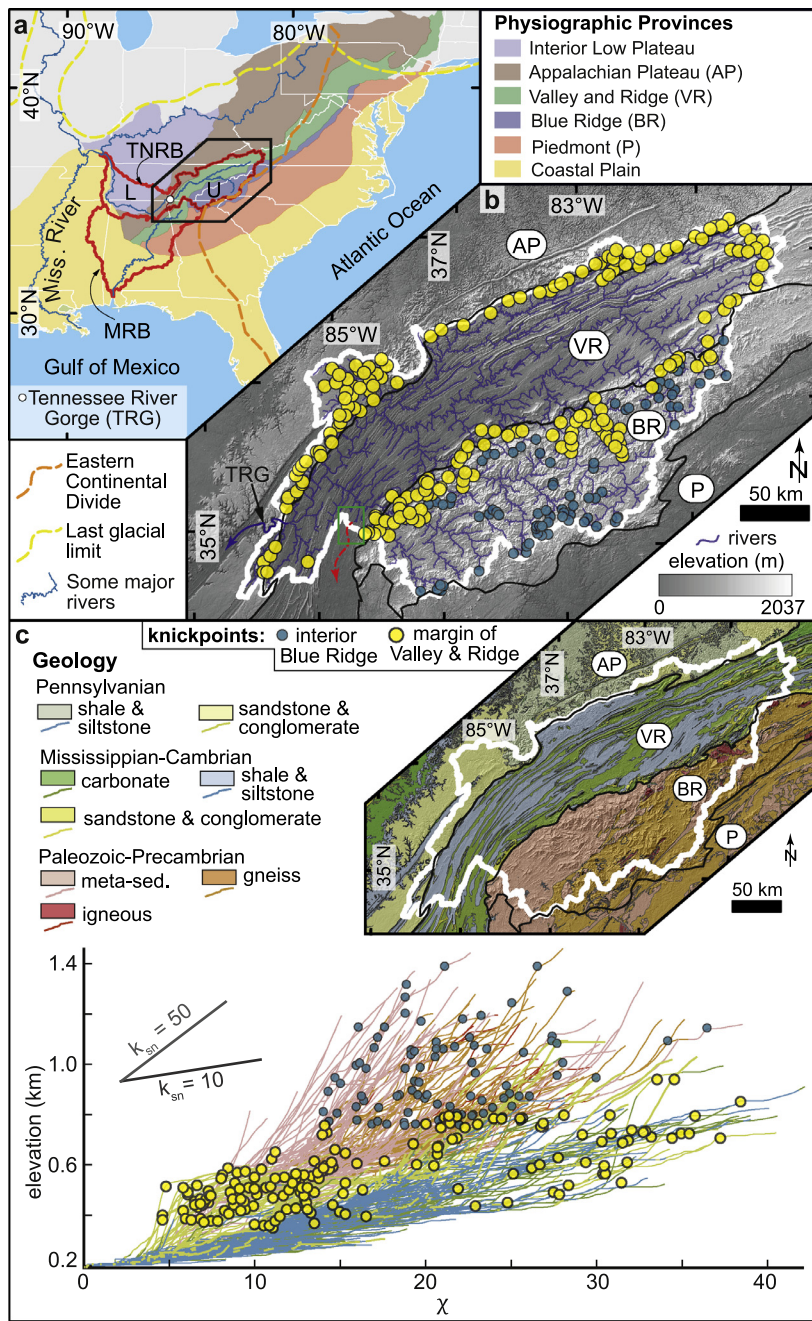


Fig. 1. Regional setting, geology, and fluvial geomorphology of the Upper Tennessee River basin. (a) Physiographic Provinces and locations of the Tennessee River Basin (TNRB) and the Mobile River Basin (MRB). The portions of the Tennessee River Basin downstream and upstream of the Tennessee River Gorge (TRG) are classified as Lower Tennessee (L) and Upper Tennessee (U) basins, respectively. The black polygon shows the location of maps in (b) and (c). (b) Topography of Upper Tennessee Basin (white polygon) with river network, knickpoints, and Physiographic Provinces (black polygons). Also noted are the locations of the modern basin outlet (blue arrow) and inferred paleo-outlet (dashed red arrow) based on the location of river terraces that cross the present-day drainage divide (green box) (Mills, 2005). (c) Simplified geologic map and Physiographic Provinces (black polygons) of the Upper Tennessee basin and corresponding χ -plot. River profiles are colored by the rock-type over which they flow. Knickpoints are classified as interior Blue Ridge (>800 m) or margin of the Valley and Ridge (~500–600 m). See Appendix B, Table S1 for descriptions of the geologic map units. (For interpretation of the colors in the figure(s), the reader is referred to the web version of this article.)

positive constants that depend on basin hydrology, channel geometry, and erosion processes (Howard, 1994; Whipple and Tucker, 1999). Equation (1) can be solved such that:

$$S = \left(\frac{E}{K} \right)^{\frac{1}{n}} A^{-(m/n)}. \quad (2)$$

Equation (2) can be integrated to predict the elevation of a river profile (Perron and Royden, 2013):

$$z(x) = z(x_b) + \left(\frac{E}{K} \right)^{\frac{1}{n}} \chi \quad (3)$$

And:

$$\chi = \int_{x_b}^x A(x')^{-m/n} dx' \quad (4)$$

where x_b is base level and χ is an integral quantity. The m/n value in equation (4) is equal to the concavity of the river. Theory and empirical studies show that the concavity of stream pro-

files in simple settings, with spatially uniform substrate, uplift, and climate falls within a small range between $\sim 0.4\text{--}0.6$ (Kirby and Whipple, 2012). Deviations from this narrow range are typically attributed to unaccounted for spatial variations in uplift, erodibility, and runoff, and there is good reason to expect that in the absence of those factors, graded rivers will exhibit concavities within this restricted range (Kirby and Whipple, 2012). Previous studies in the Appalachians show that river profile concavity is ~ 0.45 (Gallen et al., 2013; Miller et al., 2013), and this value is used for m/n to calculate χ . While there is some uncertainty in the use of this value, the intrinsic river profile concavity index is not expected to change much in the study area because variations in uplift and runoff are low, and the analysis below takes into account spatial variations in erodibility.

The transformed coordinate χ is a path integral of drainage area along a river channel and effectively linearizes river profiles in plots of χ versus elevation, or χ -plots. χ -plots are an effective visual tool for quantitative interpretation of the various factors that shape landscapes. The variable χ is usually normalized to a reference drainage area to give units of length (Perron and Royden, 2013). I present the variable as in equation (4) such that the slope of a χ -transformed river profile is the normalized steepness index (k_{sn}), a metric that is proportional to the ratio of erosion rate and the erodibility coefficient (Kirby and Whipple, 2012). Base level change is transmitted through the river network as a kinematic wave (Howard, 1994; Whipple and Tucker, 1999). Provided uniform substrate properties and uplift patterns, the wave front will propagate at the same rate both vertically and horizontally in χ -plots and river profiles will remain co-linear. Spatial variability in uplift rate or erodibility, as well as changes in drainage area through time, will effect k_{sn} and result in dispersion of χ -plots.

Numerous knickpoints – sharp changes in the slope of χ -plots – and scattered χ -transformed river profiles reveal that the Upper Tennessee basin is not in equilibrium (Figs. 1b, c). Knickpoints above ~ 800 m in elevation show no coherent, regional patterns, but are observed as local features associated with river incision along preexisting bedrock fracture zones, exhumation of locally resistant rock-types, or small-scale river captures that exploit pre-existing structures (Fig. 1c; Fig. S1). Knickpoints between $\sim 500\text{--}600$ m exhibit a stark map view pattern encircling the Valley and Ridge province, but are scattered in the Upper Tennessee River χ -plot (Figs. 1b, c). However, within individual tributary basins these knickpoints cluster in χ -plots and lie upstream of geologic contacts, suggesting that they are not geologically controlled, but propagating as a kinematic wave within tributary networks (Figs. 1b, c; Fig. S2). These observations suggest that the low elevation knickpoints ($\sim 500\text{--}600$ m) might represent the expression of a wave of incision sweeping through the basin due to a sudden base level fall, but the effects of variability in the erodibility coefficient associated with different rock-types, which can cause scatter in χ -plots, obscure this transient signal.

3.2. Erodibility and rock-type

Mills (2003) showed that a strong correlation exists between topographic form and bedrock geology in the Upper Tennessee valley, implying that the erodibility coefficient is a function of rock-type and varies spatially. Qualitatively, spatial variations in the normalized steepness index (k_{sn}) mimic changes in rock-type, as defined by a simplified geologic map, supporting Mills' (2003) interpretation (Fig. 1c). To quantify variations in the erodibility coefficient associated with different rock units, I first discretize the river network on the basis of a simplified geologic map, and using equation (3), I calculate the average normalized steepness index (k_{sn}) for each geologic map unit with a matrix inversion of χ -elevation data. Rock-type average k_{sn} varies by more than a fac-

tor of five within the basin (Figs. 1c, 2a). The high variability in k_{sn} is mostly a function of changes in the erodibility coefficient among different rock-types. This follows because both absolute and differential rates of vertical motion are expected to be low in the southeastern U.S. and will, thus, have little influence on k_{sn} , particularly at the spatial scale of Upper Tennessee basin. High lithospheric rigidity in the southeastern U.S. (effective elastic thickness of 40–60 km) dampens vertical motion due to changes in surface or subsurface loads to long wavelength, low amplitude deflections (Armstrong and Watts, 2001). Dynamic topography models indicate net subsidence in the southern Appalachians and maximum rates of differential vertical motion in the southeastern U.S. of $<4 \text{ m Ma}^{-1}$ over distances of ~ 700 km during the Cenozoic (Liu, 2014). Importantly, this low magnitude of proposed differential vertical motion is within the uncertainty of the analyses conducted therein.

It is straightforward to calculate the average erodibility coefficient, K , for each geologic map by dividing unit average k_{sn} by the average rate of erosion, provided that spatial variability in uplift is low and the stream power slope exponent, n , is equal to 1. For reasons outlined above, it is likely that spatial variability in uplift rate is negligible in the Upper Tennessee basin. Previous studies demonstrate that knickpoint migration in the Appalachians is well-explain by the steam power incision model when n is equal to 1 (Gallen et al., 2013; Miller et al., 2013), and, therefore, a value of 1 is used for n in all subsequent analyses. While previous studies and data support the simplifying that n is 1, if n were not 1, the precise values of derived parameters would change, but the general results and conclusions presented therein would still hold. To determine the erodibility coefficient for the 8 geologic map units from k_{sn} , I assume that the average erosion rate of the Upper Tennessee basin is the same as the long-term exhumation rate of the Appalachians, $27 \pm 4 \text{ m Ma}^{-1}$, which has remained consistent over a wide range of time-scales from hundreds of millions to tens of thousands of years (Boettcher and Milliken, 1994; Matmon et al., 2003). Transient portions of the landscape are included in these calculations under the assumption that the inferred long-term, average erosion rate integrates the effects of intermittent waves of transient erosion that sweep through the drainage basin, yet excluding transient river reaches has little impact on this analysis (Fig. S3).

The erodibility coefficient, as cast in equation (1), incorporates a number of effects including climatic conditions and erosional resistance, among others (Whipple, 2004). In the study area, climate conditions are relatively uniform, and thus variations in the erodibility coefficient are primarily due to differences in erosional resistance. Erosional resistance includes the effects of lithology, hydrologic roughness, and channel width (Whipple, 2004). In the Appalachians, variations in channel width, and likely hydrologic roughness, vary with lithology (Spotila et al., 2015). Given these considerations, I use the terms substrate erodibility or bedrock erodibility to describe erodibility coefficient associated with rock-type as calculated here.

Results show that the erodibility coefficient varies by more than a factor of 5 among the various rock-types in the Upper Tennessee basin, a finding consistent with independent estimates of erodibility from the Valley and Ridge (Miller et al., 2013) and Blue Ridge (Gallen et al., 2013) provinces (Fig. 2b). Rock-types with similar composition have comparable average k_{sn} and K . For example, shales and limestones in the Appalachians are compositionally alike, with varying amounts of fine-grained siliciclastics, coal, and carbonate, and both units have similar k_{sn} and K (Fig. 2; Table S1). In contrast, unit average k_{sn} and K derived from compositionally distinct rock-types, such as shales and gneisses, differ considerably (Fig. 2; Table S1). The distribution of rock-types with similar K is not random; relatively erodible shale and carbonates of the Valley

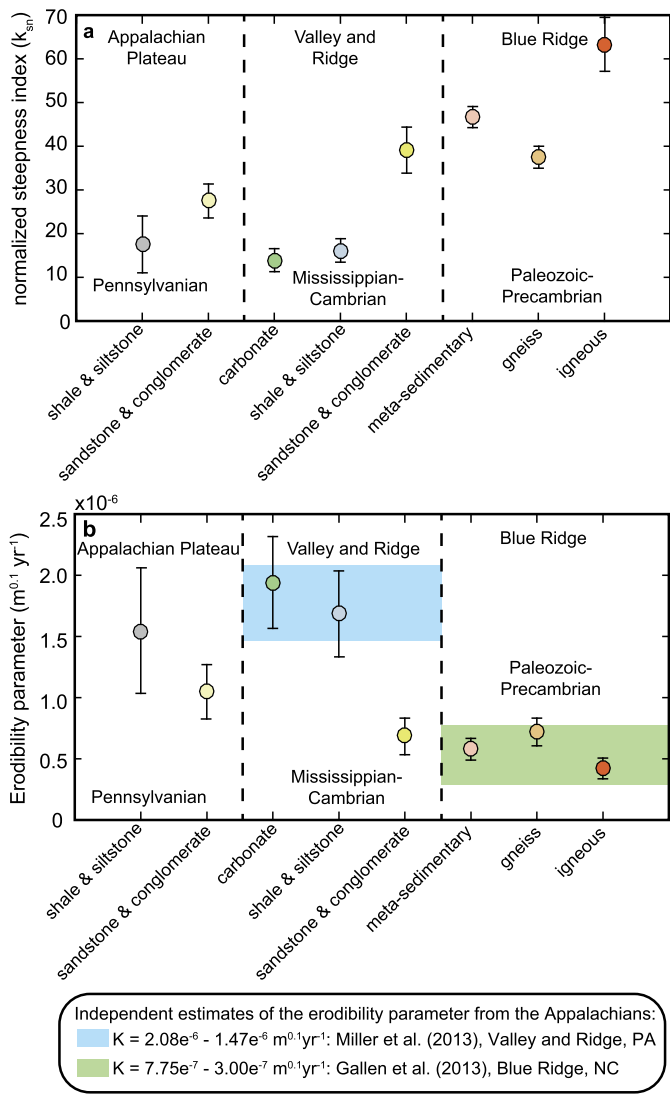


Fig. 2. Geologic unit averaged normalized steepness index (k_{sn}) for rock units in the Upper Tennessee River basin. (a) Normalized steepness index for each geologic map unit in the Upper Tennessee River basin with 1σ uncertainties. Calculation of the uncertainties accounts for autocorrelation of residuals. (b) Results from the conversion of k_{sn} to the erodibility coefficient with 1σ uncertainties determined from a Monte Carlo routine. Also shown are independent estimates of K from previous studies of Gallen et al. (2013) and Miller et al. (2013).

and Ridge province are confined to the central axis of the Upper Tennessee basin, and are flanked by relatively resistant sandstones and conglomerates of the Appalachian Plateau and metamorphic units of the Blue Ridge province (Figs. 1c, 2b). It is this variability in the erodibility coefficient that likely results in the wide scatter observed in the Upper Tennessee River basin χ -plot, and it must be accounted for to recover the base level fall history and assess the origin of the knickpoints that encircle the Valley and Ridge province (Fig. 1).

3.3. Landscape response time and base level fall history

From equation (1) the response time, τ , for a perturbation to travel from the river outlet, at $x = 0$, to a given point, x , along a river channel is given by (Whipple and Tucker, 1999):

$$\tau(x) = \int_0^x \frac{dx'}{K(x')A(x')^m} \quad (5)$$

when the slope exponent n is equal to 1. It can be seen from equation (5) that τ is similar to χ with the exception that it includes path-dependent changes in the erodibility coefficient in the denominator of the integrand. In other words, calculating τ takes into account the effects of spatial variations in the erodibility coefficient on river profile geometry. The Upper Tennessee River basin τ -plot (Fig. 3a) is more tightly clustered than the χ -plot (Fig. 1c) demonstrating that the inferred spatial pattern of erodibility explains much of the dispersion noted in the χ -transformed river profiles (Fig. S4). This analysis also emphasizes the long-response time of the Upper Tennessee River system that is nearly 40 Myr (Fig. 3).

The τ -plot provides the basis for a formal linear inversion of fluvial topography to recover the base level fall history of the Upper Tennessee basin (Pritchard et al., 2009; Roberts and White, 2010; Goren et al., 2014) (Fig. 3). Other studies that employ a similar inverse modeling approach assume that the erodibility coefficient is spatially uniform and solve for uplift as a function of space and time (Pritchard et al., 2009; Roberts and White, 2010). However, if this assumption is violated, as is the case in the southeastern U.S., it gives a biased and potentially erroneous estimate of the uplift history. For this reason, I take a different philosophical approach and assume that the erodibility coefficient is spatially variable and dictated by bedrock lithology, and that spatial variability in rock uplift rate (or base level fall rate) is negligible, but varies in time. I employ the inverse approach of Goren et al. (2014), which is based on equation (1), to recover the base level fall history of the Upper Tennessee River basin (Appendix A). To quantify the uncertainties associated with inputs into the linear inverse model (e.g. k_{sn} and average erosion rate), I employ a Monte Carlo routine with 1000 independent simulations. For each simulation, a k_{sn} value and average erosion rate is randomly selected based on the mean and standard deviation, assuming a Gaussian distribution of uncertainties, for each geologic map unit based on its measured k_{sn} and the inferred long-term average erosion rate ($27 \pm 4 \text{ m Ma}^{-1}$). The inferred k_{sn} and erosion rate from each simulation are used to calculate the erodibility coefficient for each rock unit and the response time of the river, τ , using equation (5), and the τ -elevation data is then inverted for the base level fall history.

The inverse modeling results show that the lower knickpoints (~ 500 – 600 m) represent the propagating front of transient incision resulting from a rapid ~ 150 m drop in base level at $\sim 9 \pm 3$ Ma, which rejuvenated topography and enhanced erosion rates in the basin (Fig. 3; Fig. S5). A single, rapid base level fall event is consistent with capture of the hypothesized Appalachian River by the Lower Tennessee River (Hayes and Campbell, 1894). The inference is that the upper portion of the Appalachian River was captured by the paleo-Lower Tennessee River in the Late Miocene diverting it westward into the modern Lower Tennessee River system from a more direct southerly route to the Gulf of Mexico through the Mobile basin.

The interpreted kinematics and timing of capture are corroborated by independent geological and biological evidence. Fluvial terraces preserved along the present-day drainage divide between the Upper Tennessee and Mobile basins support the interpretation of capture of the Appalachian River, but absolute age control on these deposits is lacking (Mills, 2005) (Fig. 1b). The timing and direction of river network topological changes are consonant with observed shifts in the rates and patterns of sediment dispersal to the Gulf of Mexico (Galloway et al., 2011). Phylogenetic studies document the biological expression of river capture as a major divergence event of freshwater fishes at ~ 9 Ma and of salamanders at ~ 7 Ma in the Upper Tennessee and Mobile basins (Near and Keck, 2005; Kozak et al., 2006). The concordance of the inferred timing of river capture determined from the geomorphic record

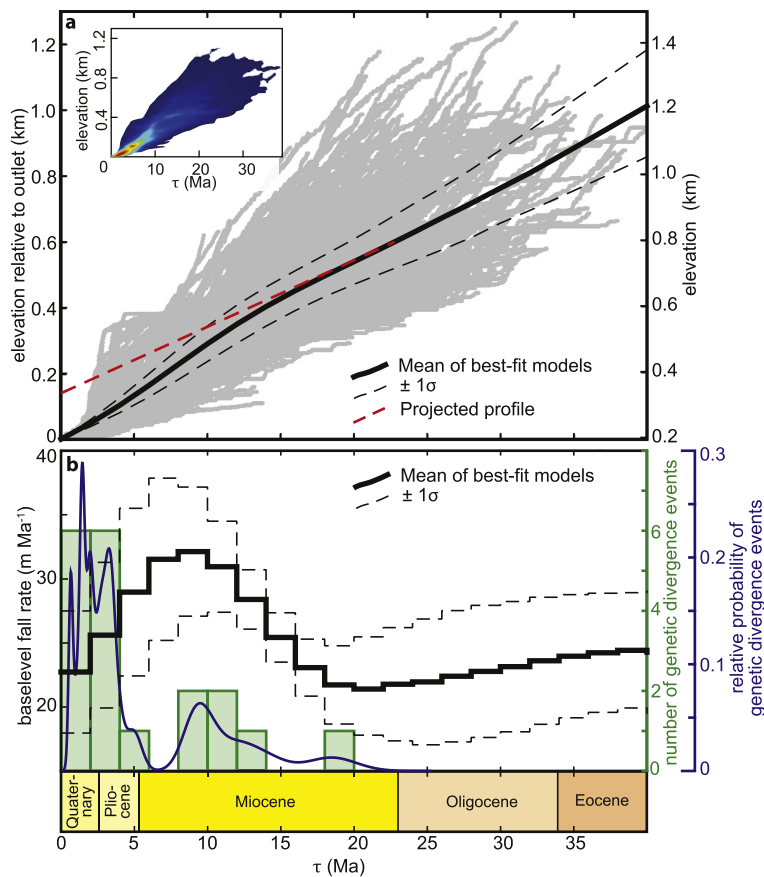


Fig. 3. Upper Tennessee Basin τ -plot and linear inverse model results. (a) River response time (τ) versus elevation with the mean ($\pm 1\sigma$) of best-fit inverse models derived from a Monte Carlo routine. The projected profile demonstrates the magnitude of base level drop, ~ 150 m. Inset shows relative data point density (red-high, blue-low). (b) Mean $\pm 1\sigma$ of best-fit base level fall rate history from inverse modeling Monte Carlo routine. The results best describe a single, rapid base level fall event at 9 ± 3 Ma. The number (green histogram) and relative probability (blue line) of genetic divergence events of *Nothonotus* Darters in the southeastern U.S. (Near and Keck, 2005) are shown. The increase in the number of divergence events < 5 Ma is attributed to Plio-Pleistocene climate change and the Late Miocene spike correlates with the timing of river capture.

and the genes of aquatic species suggests that the DNA of living species can be utilized as a geochronological tool. Alternatively, well constrained changes in the geomorphic system might be exploited as a means to calibrate genetic mutation rates in aquatic species. Importantly, a spike in the number of divergence events of *Nothonotus* Darters in the southeastern U.S. is temporally coincident with capture of the Appalachian River (Near and Keck, 2005) (Fig. 3b), and implies that the process(es) driving river capture act to enhance speciation.

4. Mechanisms driving river capture

My results, combined with existing geological and biological data, demonstrate that capture of the Appalachian River occurred more than 100 million years after the last phase of tectonism (Hatcher, 1989) and several million years prior to the transition to a cooler, more rapidly fluctuating Quaternary-like climate that initiated ~ 3 – 4 Ma (Molnar and England, 1990). This suggests that tectonics and climate change are not responsible for driving capture of the Appalachian River. Most dynamic topography models predict low rates of subsidence (maximum rates typically < 5 $m\text{Ma}^{-1}$) in the study area during the Cenozoic (Liu, 2014; Rowley et al., 2013). Furthermore, it is difficult to reconcile the observations presented in this study with the slow and long-wavelength nature of uplift resulting from dynamic topography or flexural isostasy expected in the southeastern U.S. Instead, I argue that changes in bedrock erodibility plays an important, but unappreciated role in the dynamics of post-orogenic landscapes because

spatial and temporal changes in rock strength (e.g. erodibility) will be common in decaying orogens. Below, I explore the viability of changing bedrock erodibility as an autogenic driver for capture of the Appalachian River.

4.1. Rock-type averaged normalized steepness index (k_{sn}) and erodibility

It is first important to demonstrate that substrate erodibility has changed in the paleo-Lower Tennessee drainage basin to shift boundary conditions to favor capture of the Appalachian River. As argued above, geologic unit average k_{sn} can serve as a proxy for bedrock erodibility in the southeastern U.S. I calculate average k_{sn} for 16 different geologic map units that span the modern Tennessee and Mobile drainage basins, which roughly cover the footprint of the paleo-Lower Tennessee–Appalachian River systems (Fig. 4). Rock-type average k_{sn} varies by approximately a factor of 6 throughout the southeastern U.S., consistent with the smaller scale analysis conducted for the Upper Tennessee River basin (Figs. 2, 4). The Lower and Upper Tennessee basins are connected by the Tennessee River Gorge that cuts through a resistant sandstone and conglomerate capstone (Fig. S6). Importantly, this capstone once covered the Appalachian and Interior Low Plateaus, spanning nearly the entire contemporary Lower Tennessee River system (Figs. 1a, c; 4a). The average k_{sn} of the capstone is more than a factor of 2 higher than the underlying shale and carbonate units, and indicates that the paleo-Lower Tennessee River network

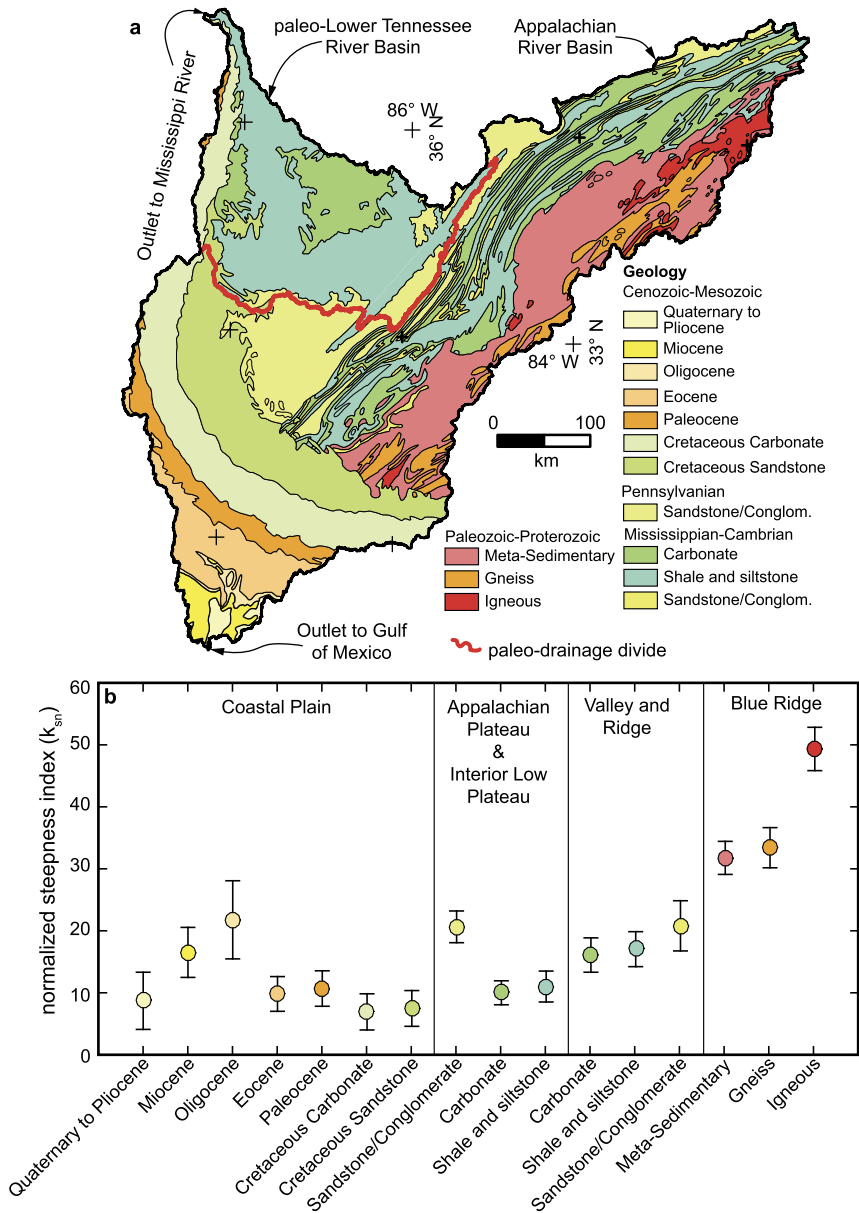


Fig. 4. Simplified geologic map of the paleo-Little Tennessee and Appalachian River basins and geologic unit averaged normalized steepness index. (a) Simplified geologic map covering the modern Tennessee and Mobile River basins shown in Fig. 1a. The modeled drainage divide between the paleo-Little Tennessee and Appalachian River basins is shown in red. (b) The normalized steepness index (k_{sn}) (mean $\pm 1\sigma$) for the 16 geologic map units shown in a. The normalized steepness index for each geologic map unit was calculated using a matrix inversion of χ -elevation data derived from 3-arc second SRTM digital topography. Note minor differences in k_{sn} relative to Fig. 2 are due to using DEMs of different resolutions and calculations conducted over different spatial extents.

experienced a major increase in erodibility as the capstone was eroded (Fig. 4b).

4.2. Drainage basin response to variations in substrate erodibility

To assess the influence of erosion of the capstone and exposure of underlying, more erodible shale and carbonate rock units on the evolution of the Tennessee River basin, I synthetically dam the Tennessee River Gorge to model the drainage pattern prior to capture. Using the modeled paleo-drainage system, I calculate the steady-state river network elevations assuming two different erodibility patterns: one where the capstone is present throughout the Appalachian and Interior Low Plateaus, and another, based on the modern geology, where it is largely absent due to erosion (Fig. 5). Here, calculation of the steady-state river elevation relies on the topology of the modeled drainage network and the average k_{sn} calculated from the 16 geologic map units (Reed et al.,

2005) (Figs. 4, 5). Predicted steady-state river network elevation maps can identify theoretically unstable drainage divides and directions of divide motion (Willett et al., 2014). Drainage divides separating channel heads with contrasting steady-state elevations are unstable and shift, through divide migration or river capture, in the direction of higher channel elevation due to erosional asymmetry across the divide (Willett et al., 2014).

Substrate erodibility drops by more than a factor of two when the Appalachian Plateau capstone is eroded, imposing new boundary conditions on the paleo-Lower Tennessee River network. The decrease in erodibility forces river channel gradients and elevations to decline. The concomitant decrease in channel head elevations pushes the paleo-Lower Tennessee basin from a state of net drainage area loss to one where it is largely expanding at the expense of neighboring basins (Fig. 5; Fig. S7). Incision through the capstone drops the paleo-Lower Tennessee River channel head

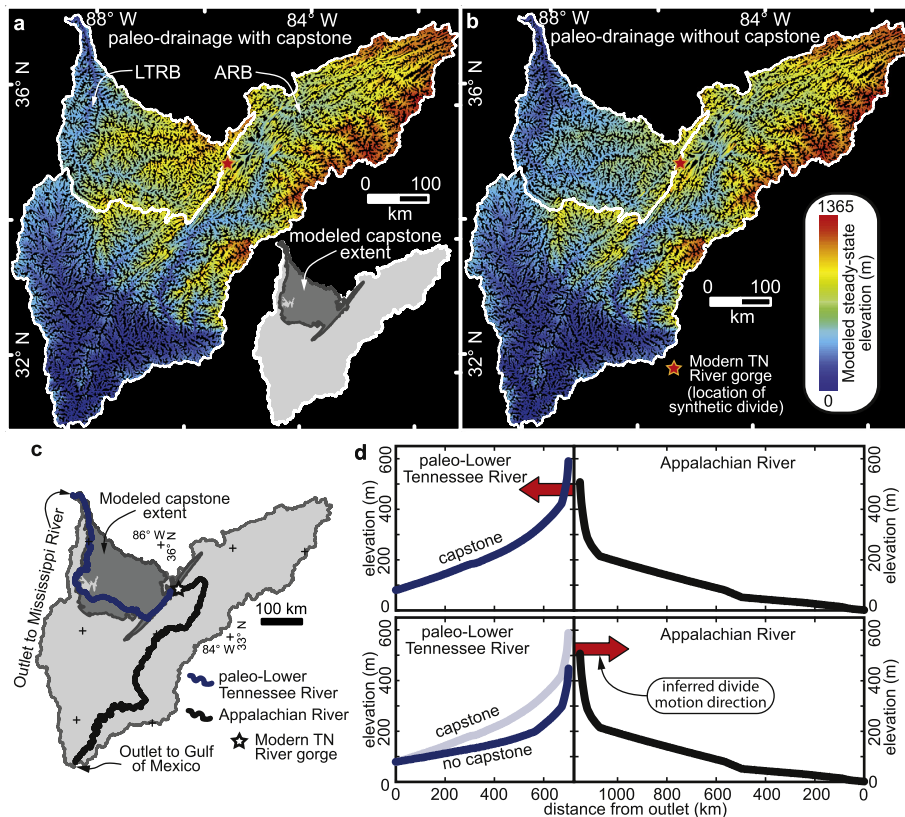


Fig. 5. Steady-state elevations for the modeled paleo-Little Tennessee River basin (LTRB) and Appalachian River basin (ARB) drainage networks. (a) Map of mean steady-state elevations assuming a capstone extended across the entire foreland basin. (b) Same as a, but using the modern distribution of rock-types where the capstone is largely eroded. The outlines of the simulated drainage basins are represented by the white polygons in a and b. The 1σ uncertainties associated with predicted elevations are shown in Fig. S7. (c) Map showing the location of the modeled paleo-Little Tennessee and the Appalachian rivers; they meet at the synthetic divide (star). (d) Modeled steady-state profiles of the paleo-Little Tennessee and Appalachian rivers with (upper panel) and without (lower panel) a capstone. Channel elevations are the mean from a Monte Carlo routine. The 1σ uncertainties are less than the line thickness.

elevation by ~ 150 m, enough to reverse the divide motion direction at the location of modern Tennessee River Gorge, and facilitate capture of the Appalachian River (Fig. 5). The reduction in river gradient forced by increased discharge following capture drops channel elevations by ~ 150 m at the Tennessee River Gorge, consistent with the amount of base level lowering observed in the Upper Tennessee basin today (Figs. 3, 6).

This analysis indicates that capture of the Appalachian River was facilitated simply by erosion of a resistant capstone in the ancient foreland basin and exposure of underlying more erodible rock-types. These results imply that, despite a nearly 1000 km longer travel distance, the more optimal path for the modern Upper Tennessee River to the Gulf of Mexico is via the Mississippi drainage basin, rather than the shorter southerly route through the Mobile drainage basin. These findings demonstrate that major late Cenozoic geologic and evolutionary events in the southeastern U.S., and possibly other post-orogenic mountain ranges, might be simply explained by the autogenic landscape response to exhumation of rock-types of variable strength.

5. Implications for the co-evolution of landscapes and aquatic species in ancient mountain belts

Rock-types of variable erodibility will be continually exhumed to the Earth's surface through erosion. Spatial and temporal changes in bedrock erodibility will drive autogenic transient landscape evolution, dynamically reshape drainage basins and propel aquatic species evolution long after the cessation of tectonics. When incising through less erodible (more resistant) into more erodible rock, rivers cut down faster into the more erodible units,

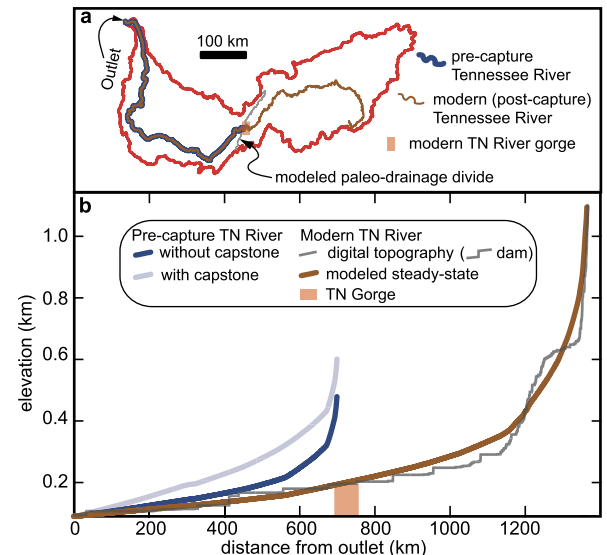


Fig. 6. Modeled changes in elevation due to river capture. (a) Map showing the locations of the longitudinal river profiles shown in b and the location of the Tennessee River Gorge within the context of the Tennessee River basin (red polygon). (b) River longitudinal river profiles for the pre-capture Tennessee River with and without a capstone. The modern (post-capture) Tennessee River from a DEM and modeled steady-state elevation based on the normalized steepness index (k_{sn}) derived from a simplified geologic map are also shown.

which steepens channels near contacts between the more erodible rock downstream and the more resistant rock upstream. This facil-

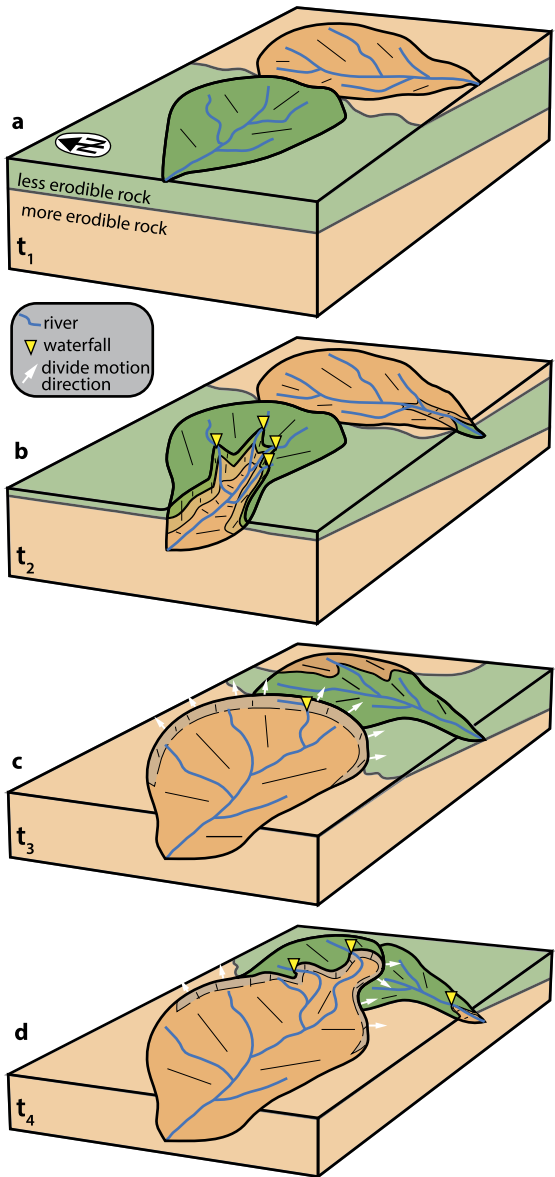


Fig. 7. Conceptual model showing the evolution of two adjacent drainage basins as one basin transitions from a less erodible to a more erodible rock and the other from a more erodible to a less erodible rock with steady base level fall rate at the basin outlets. (a) (t_1) initial condition. (b) (t_2) River gradients decrease in the basin that incises from less erodible to more erodible rock. This results in the formation of waterfalls (vertical knickpoints) that can act as barriers to upstream migration of genetic information for aquatic species (Rahel, 2007). River gradients increase in the basin eroding from more to less erodible rock. (c) (t_3) The change in river network gradients promotes an elevation contrast and erosional asymmetry along the local divide that fosters expansion of the drainage basin incising the more erodible rock and contraction of the basin eroding less erodible rock. (d) (t_4) Drainage divide motion occurs through progressive retreat and discrete river capture, facilitating aquatic species dispersal and vicariance events.

itates the formation of vertical knickpoints (e.g. waterfalls) (Forte et al., 2016) that can act as genetic barriers to upstream gene flow (Rahel, 2007) (Fig. 7a, b). Furthermore, the associated reduction in steady-state channel head elevations ultimately fosters asymmetric erosion rates across drainage divides that favor channel lengthening and drainage basin expansion (Fig. 7c). Conversely, incision from more to less erodible rock-types steepens and elevates river channels, promoting the shortening of rivers and contraction of drainage basins (Fig. 7c, d). Drainage basin expansion and contraction will occur through progressive drainage divide migration and discrete river capture events. Both processes facilitate aquatic

species dispersal and vicariance events. Lithologically-triggered transient landscape evolution, thus, acts to increase the number of aquatic species divergence events, helping to elevate biodiversity in tectonically quiescent settings.

The effects of rock-type on landscape dynamics will be most pronounced in layered sub-horizontal rocks (Forte et al., 2016), such as the foreland basins of ancient mountain belts. Foreland basin stratigraphy can alternate from more resistant coarse-grained siliciclastic units to more erodible fine-grained siliciclastic and carbonate rocks and vice versa. Erosion of the sub-horizontal strata common in foreland basins will intermittently impose new boundary conditions over large expanses of the landscape, forcing channel gradients to change and altering landscape response times. The ensuing response can result in a cascading effect, impacting geomorphic, stratigraphic, and biologic systems for tens of millions of years, as illustrated by the late Cenozoic history of the Tennessee River basin. The ongoing exhumation of rocks of variable strength coupled with the sluggish response of river systems suggests that it is unlikely that post-orogenic landscapes will ever reach a steady-state or equilibrium between rock uplift and erosion on regional scales. Importantly, these findings demonstrate that evidence of landscape unsteadiness is not uniquely indicative of external drivers, such as uplift associated with mantle dynamics or climate change, but rather can be a characteristic feature of decaying orogens.

Climate change and/or uplift due to dynamic topography might be the dominant driver of landscape unsteadiness in some tectonically quiescent settings. In such cases, the external forcing must be significant enough to overwhelm intrinsic variability associated with substrate erodibility. This seems unlikely in the Appalachians, where the erodibility coefficient varies by more than a factor of 5 among the different rock-types. Changes in climate will force a transient landscape response that is filtered through existing variations in substrate erodibility. Changes in rock uplift rate would need to exceed a factor of 5 to compete with variations in erodibility in the southeastern U.S., which for reasons discussed earlier is unlikely. However, in settings where spatial variability in substrate erodibility is low and horizontal contacts, which amplify the impact of erodibility on unsteady erosion (Forte et al., 2016), are minimal or absent, it is possible that external drivers are primarily responsible for evidence of post-orogenic landscape unsteadiness. For example, cratons or ancient orogenic cores and volcanic arcs, which are largely comprised of crystalline rocks and mostly devoid of horizontal layering, are setting where the role of rock-type can be minimized and provide the best opportunity to assess the potential role of climate or dynamic topography on landscape evolution. Nonetheless, it is important to recognize that neither rock-type, climate change, nor uplift from dynamic mantle processes are mutually exclusive models, all can act in concert to drive topographic change. Further research is needed to quantify and untangle the influence of these different drivers on the evolution of post-orogenic landscapes. Only then will we come to a complete understanding of the dynamics of ancient mountain settings and the associated implications for geomorphic, stratigraphic, and biological archives.

6. Conclusions

The results of this study confirm that spatial variations in topographic form and river channel steepness can be explained by changes in the erodibility coefficient of different rock units. The erodibility coefficient in the southeastern U.S. varies by more than a factor of 5 among different rock-types and strongly influences landscape response times. The Upper Tennessee River basin is in a transient state of adjustment to a ~ 150 m base level fall event that occurred at $\sim 9 \pm 3$ Ma, consistent with the timing of

phylogenetic change in aquatic species and the dispersal of sediment to offshore basins (Near and Keck, 2005; Kozak et al., 2006; Galloway et al., 2011). This study demonstrates that variable substrate erodibility represents an important, yet underappreciated, player in the dynamics of ancient mountain landscapes. My findings suggest that capture of the Appalachian River, and the associated biological and sedimentary consequences, is the result of expansion of the paleo-Little Tennessee basin in response to new boundary conditions imposed as the river network eroded from a resistant capstone into more erodible shales and carbonates. More generally, the results of this study show that evidence of unsteady post-orogenic landscape evolution is not uniquely indicative of external drivers, such as geodynamic or climate forcing, as is typically the interpretation. Instead, these results favor a new model of inherently dynamic and unsteady landscape evolution due to the continued exhumation of rocks of variable strength that fosters landscape disequilibrium and the reshaping of river networks. These results have potentially important implications for interpreting stratigraphic records in offshore basins and elucidating the geo-logic processes that pressure the evolution and diversity of aquatic species in tectonically quiescent regions.

Author contributions

S.F.G. conceived of the study, performed the data analysis, and wrote the manuscript.

Data availability

The digital elevation model data and the digital geologic maps that support the findings of this study are available through the U.S. Geological Survey at earthexplorer.usgs.gov and ngmdb.usgs.gov, respectively.

Acknowledgements

This work benefited from discussions with Sean Willett and Emanuele Giachetta and advice from Liran Goren on the inverse modeling of fluvial topography. The author would like to thank Frank J. Pazzaglia, Karl W. Wegmann, Scott R. Miller, Jeremy K. Caves, Peter van der Beek, Gareth Roberts, and an anonymous reviewer for informal and formal reviews of an earlier version of this manuscript. Greg Hancock and an anonymous reviewer are thanked for thorough and thought-provoking reviews that substantially improved the final version of this manuscript.

Appendix A. Linear inverse modeling

Assuming $n = 1$ in equation (1), I perform a linear inversion of the Upper Tennessee River network to recover the history of base level fall following the approach of Goren et al. (2014) (Fig. 2). Assuming a block uplift (or base level fall) scenario, the elevation of the river network can be cast as:

$$z(x) = \int_{-\tau(x)}^0 U(t') dt' \quad (6)$$

where t' is an integration variable, time zero is the present, and the past is represented by negative time. Equation (6) predicts that the present elevation of a given point along a river network, $z(x)$, is the integral of the relative uplift rate along the downstream channel points during the past over a duration of $\tau(x)$ and that all tributaries with the same $\tau(x)$ will lie at the same elevation $z(x)$.

For this inverse exercise, my goal is to recover the rate of uplift (or base level fall) from the river network during discrete time intervals using equation (6). The data are organized such that there

are N data points of z and τ along the fluvial network that share a common uplift history and are ordered according to elevation. A time step of constant length, ΔT , is chosen that will determine the number of discrete time intervals, q . In this case, ΔT is chosen as 2 Ma, but changing this variable has little effect on the general model outcome. The exact discrete version of equation (6) will depend on the chosen time step length and the number of data points in the fluvial network.

Using the discretization described above, equation (6) can be written for each data point and the equations can be organized in matrix form:

$$\mathbf{AU} = \mathbf{z} \quad (7)$$

where \mathbf{A} is an $N \times q$ matrix and \mathbf{z} is elevation. This is an over-determined inverse problem as there are more known data points than unknown parameters. As such, a least squares estimate for \mathbf{U} is used (Tarantola, 1987):

$$\mathbf{U} = \mathbf{U}_{\text{pri}} + (\mathbf{A}^T \mathbf{A} + \Gamma^2 \mathbf{I})^{-1} \mathbf{A}^T (\mathbf{z} - \mathbf{AU}_{\text{pri}}) \quad (8)$$

where $\mathbf{U}_{\text{pri}} = (1/N) \sum_{i=1}^N (z_i / \sum_{j=1}^q \mathbf{A}_{i,j})$ and is a prior guess at the uplift rate, Γ is a dampening coefficient that determines the smoothness imposed on the solution, and \mathbf{I} is the $q \times q$ identity matrix.

Appendix B. Supplementary material

Supplementary material related to this article can be found online at <https://doi.org/10.1016/j.epsl.2018.04.029>.

References

- Armstrong, G.D., Watts, A.B., 2001. Spatial variations in Te in the southern Appalachians, eastern United States. *J. Geophys. Res., Solid Earth* 106, 22009–22026. <https://doi.org/10.1029/2001JB000284>.
- Battin, T.J., Kaplan, L.A., Findlay, S., Hopkinson, C.S., Marti, E., Packman, A.I., Newbold, J.D., Sabater, F., 2008. Biophysical controls on organic carbon fluxes in fluvial networks. *Nat. Geosci.* 1, 95–100. <https://doi.org/10.1038/ngeo101>.
- Biryol, C.B., Wagner, L.S., Fischer, K.M., Hawman, R.B., 2016. Relationship between observed upper mantle structures and recent tectonic activity across the Southeastern United States. *J. Geophys. Res., Solid Earth* 121, 3393–3414. <https://doi.org/10.1002/2015JB012698>.
- Boettcher, S.S., Milliken, K.L., 1994. Mesozoic–Cenozoic unroofing of the southern Appalachian Basin: apatite fission track evidence. *J. Geol.* 102, 655.
- Davis, W.M., 1899. The geographical cycle. *Geogr. J.* 14, 481–504. <https://doi.org/10.2307/1774538>.
- Etnier, D.A., Starnes, W.C., 1993. *The Fishes of Tennessee*. University of Tennessee Press, Knoxville, Tennessee.
- Forte, A.M., Yanites, B.J., Whipple, K.X., 2016. Complexities of landscape evolution during incision through layered stratigraphy with contrasts in rock strength. *Earth Surf. Process. Landf.* 41, 1736–1757. <https://doi.org/10.1002/esp.3947>.
- France-Lanord, C., Derry, L.A., 1997. Organic carbon burial forcing of the carbon cycle from Himalayan erosion. *Nature* 390, 65–67. <https://doi.org/10.1038/36324>.
- Gallen, S.F., Wegmann, K.W., Bohnenstiel, D.R., 2013. Miocene rejuvenation of topographic relief in the southern Appalachians. *GSA Today* 23, 4–11. <https://doi.org/10.1130/GSATG163A.1>.
- Galloway, W.E., Whiteaker, T.L., Ganey-Curry, P., 2011. History of Cenozoic North American drainage basin evolution, sediment yield, and accumulation in the Gulf of Mexico basin. *Geosphere* 7, 938–973. <https://doi.org/10.1130/ges00647.1>.
- Goren, L., Fox, M., Willett, S.D., 2014. Tectonics from fluvial topography using formal linear inversion: theory and applications to the Inyo Mountains, California. *J. Geophys. Res., Earth Surf.* 119, 1651–1681. <https://doi.org/10.1002/2014JF003079>.
- Gunnell, Y., Harbor, D.J., 2010. Butte detachment: how pre-rift geological structure and drainage integration drive escarpment evolution at rifted continental margins. *Earth Surf. Process. Landf.* 35, 1373–1385. <https://doi.org/10.1002/esp.1973>.
- Hack, J.T., 1960. Interpretation of erosional topography in humid temperate regions. *Am. J. Sci.* 258-A, 80–97. Bradley Volume.
- Hancock, G., Kirwan, M., 2007. Summit erosion rates deduced from ^{10}Be : implications for relief production in the central Appalachians. *Geology* 35, 89–92. <https://doi.org/10.1130/g23147a.1>.

- Hatcher, R.D.J., 1989. Tectonic synthesis of the U.S. Appalachians. In: Hatcher, R.D.J., Thomas, W.A., Viele, G.W. (Eds.), *The Appalachian-Ouachita Orogen in the United States*. The Geological Society of America, Boulder, CO, pp. 511–531.
- Hayes, C.W., Campbell, M.R., 1894. Geomorphology of the southern Appalachians. *Natl. Geogr. Mag.* 6, 63–126.
- Hoorn, C., Wesselingh, F.P., ter Steege, H., Bermudez, M.A., Mora, A., Sevink, J., Sanmartín, I., Sanchez-Meseguer, A., Anderson, C.L., Figueiredo, J.P., Jaramillo, C., Riff, D., Negri, F.R., Hooghiemstra, H., Lundberg, J., Stadler, T., Särkinen, T., Antonelli, A., 2010. Amazonia through time: Andean uplift, climate change, landscape evolution, and biodiversity. *Science* 330, 927–931. <https://doi.org/10.1126/science.1194585>.
- Howard, A.D., 1994. A detachment-limited model of drainage basin evolution. *Water Resour. Res.* 30, 2261–2285. <https://doi.org/10.1029/94wr00757>.
- Johnson, D.W., 1905. The Tertiary history of the Tennessee river. *J. Geol.* 13, 194–231.
- Kirby, E., Whipple, K.X., 2012. Expression of active tectonics in erosional landscapes. *J. Struct. Geol.* 44, 54–75. <https://doi.org/10.1016/j.jsg.2012.07.009>.
- Kozak, K.H., Blaine, R.A., Larson, A., 2006. Gene lineages and eastern North American palaeodrainage basins: phyleogeography and speciation in salamanders of the Eurycea bislineata species complex. *Mol. Ecol.* 15, 191–207. <https://doi.org/10.1111/j.1365-294X.2005.02757.x>.
- Liu, L., 2014. Rejuvenation of Appalachian topography caused by subsidence-induced differential erosion. *Nat. Geosci.* 7, 518–523. <https://doi.org/10.1038/ngeo2187>.
- Matmon, A., Bierman, P.R., Larsen, J., Southworth, S., Pavich, M., Caffee, M., 2003. Temporally and spatially uniform rates of erosion in the southern Appalachian Great Smoky Mountains. *Geology* 31, 155–158. [https://doi.org/10.1130/0091-7613\(2003\)031<0155:tasuro>2.0.co;2](https://doi.org/10.1130/0091-7613(2003)031<0155:tasuro>2.0.co;2).
- Mayden, R.L., 1988. Vicariance biogeography, parsimony, and evolution in North American freshwater fishes. *Syst. Biol.* 37, 329–355. <https://doi.org/10.1093/sysbio/37.4.329>.
- Miller, S.R., Sak, P.B., Kirby, E., Bierman, P.R., 2013. Neogene rejuvenation of central Appalachian topography: evidence for differential rock uplift from stream profile files and erosion rates. *Earth Planet. Sci. Lett.* 369–370, 1–12. <https://doi.org/10.1016/j.epsl.2013.04.007>.
- Milliman, J.D., Syvitski, J.P.M., 1992. Geomorphic/tectonic control of sediment discharge to the ocean: the importance of small mountainous rivers. *J. Geol.* 100, 525–544. <https://doi.org/10.1086/629606>.
- Mills, H.H., 2003. Inferring erosional resistance of bedrock units in the east Tennessee mountains from digital elevation data. *Geomorphology* 55, 263–281. [https://doi.org/10.1016/S0169-555X\(03\)00144-2](https://doi.org/10.1016/S0169-555X(03)00144-2).
- Mills, H.H., 2005. Relative-age dating of transported regolith and application to study of landform evolution in the Appalachians. *Geomorphology* 67, 63–96. <https://doi.org/10.1016/j.geomorph.2004.08.015>.
- Mills, H.H., Kaye, J.M., 2001. Drainage history of the Tennessee River: review and new metamorphic quartz gravel locations. *Southeast. Geol.* 40, 75–97.
- Molnar, P., England, P., 1990. Late Cenozoic uplift of mountain ranges and global climate change: chicken or egg? *Nature* 346, 29–34. <https://doi.org/10.1038/346029a0>.
- Naeser, C.W., Naeser, N.D., Newell, W.L., Southworth, S., Edwards, L.E., Weems, R.E., 2016. Erosional and depositional history of the Atlantic passive margin as recorded in detrital zircon fission-track ages and lithic detritus in Atlantic Coastal plain sediments. *Am. J. Sci.* 316, 110–168. <https://doi.org/10.2475/02.2016.02>.
- Near, T.J., Keck, B.P., 2005. Dispersal, vicariance, and timing of diversification in *Nothonotus* darters. *Mol. Ecol.* 14, 3485–3496. <https://doi.org/10.1111/j.1365-294X.2005.02671.x>.
- Pazzaglia, F.J., Brandon, M.T., 1996. Macrogeomorphic evolution of the post-Triassic Appalachian mountains determined by deconvolution of the offshore basin sedimentary record. *Basin Res.* 8, 255–278. <https://doi.org/10.1046/j.1365-2117.1996.00274.x>.
- Perron, J.T., Royden, L., 2013. An integral approach to bedrock river profile analysis. *Earth Surf. Process. Landf.* 38, 570–576. <https://doi.org/10.1002/esp.3302>.
- Pritchard, D., Roberts, G.G., White, N.J., Richardson, C.N., 2009. Uplift histories from river profiles. *Geophys. Res. Lett.* 36. <https://doi.org/10.1029/2009GL040928>.
- Rahel, F.J., 2007. Biogeographic barriers, connectivity and homogenization of freshwater faunas: it's a small world after all. *Freshw. Biol.* 52, 696–710. <https://doi.org/10.1111/j.1365-2427.2006.01708.x>.
- Raymo, M.E., Ruddiman, W.F., 1992. Tectonic forcing of late Cenozoic climate. *Nature* 359, 117–122. <https://doi.org/10.1038/359117a0>.
- Reed, J.C., Wheeler, J.O., Tucholke, B.E., Stettner, W.R., Soller, D.R., 2005. Decade of North American Geology Geologic Map of North America—Perspectives and Explanation. Geological Society of America, Boulder, Colorado.
- Roberts, G.G., White, N., 2010. Estimating uplift rate histories from river profiles using African examples. *J. Geophys. Res., Solid Earth* 115. <https://doi.org/10.1029/2009JB006692>.
- Rowley, D.B., Forte, A.M., Moucha, R., Mitrovica, J.X., Simmons, N.A., Grand, S.P., 2013. Dynamic topography change of the Eastern United States since 3 million years ago. *Science* 340, 1560–1563. <https://doi.org/10.1126/science.1229180>.
- Schwanghart, W., Scherler, D., 2014. Short communication: TopoToolbox 2 – MATLAB-based software for topographic analysis and modeling in Earth surface sciences. *Earth Surf. Dyn.* 2, 1–7. <https://doi.org/10.5194/esurf-2-1-2014>.
- Simpson, C.T., 1900. On the evidence of the unionidae regarding the former courses of the Tennessee and other southern rivers. *Science* 12, 133–136.
- Spotila, J.A., Moskey, K.A., Prince, P.S., 2015. Geologic controls on bedrock channel width in large, slowly-eroding catchments: case study of the New River in eastern North America. *Geomorphology* 230, 51–63. <https://doi.org/10.1016/j.geomorph.2014.11.004>.
- Summerfield, M.A., Hulton, N.J., 1994. Natural controls of fluvial denudation rates in major world drainage basins. *J. Geophys. Res., Solid Earth* 99, 13871–13883. <https://doi.org/10.1029/94JB00715>.
- Tarantola, A., 1987. *Inverse Problem Theory: Methods for Data Fitting and Parameter Estimation*. Elsevier, Amsterdam.
- Tucker, G.E., van der Beek, P., 2013. A model for post-orogenic development of a mountain range and its foreland. *Basin Res.* 25, 241–259. <https://doi.org/10.1111/j.1365-2117.2012.00559.x>.
- Waters, J.M., Craw, D., Youngson, J.H., Wallis, G.P., 2001. Genes meet geology: fish phylogeographic pattern reflects ancient, rather than modern, drainage connections. *Evolution* 55, 1844–1851. <https://doi.org/10.1111/j.0014-3820.2001.tb00833.x>.
- Whipple, K.X., 2004. Bedrock rivers and the geomorphology of active orogens. *Annu. Rev. Earth Planet. Sci.* 32, 151–185. <https://doi.org/10.1146/annurev.earth.32.101802.120356>.
- Whipple, K.X., Tucker, G.E., 1999. Dynamics of the stream-power river incision model: implications for height limits of mountain ranges, landscape response timescales, and research needs. *J. Geophys. Res., Solid Earth* 104, 17661–17674. <https://doi.org/10.1029/1999JB900120>.
- Willett, S.D., McCoy, S.W., Perron, J.T., Goren, L., Chen, C.-Y., 2014. Dynamic reorganization of river basins. *Science* 343. <https://doi.org/10.1126/science.1248765>.